Bioconjugate Chemistry

COMMUNICATION

pubs.acs.org/bc

Aromatic Aldehyde and Hydrazine Activated Peptide Coated Quantum Dots for Easy Bioconjugation and Live Cell Imaging

Gopal Iyer,[*,§,†] Fabien Pinaud,[*,‡,§] Jianmin Xu,[†] Yuval Ebenstein,[†] Jack Li,[†] Jessica Chang,[†] Maxime Dahan,[‡] and Shimon Weiss[*,†]

[†]Department of Chemistry and Biochemistry, California NanoSystems Institute, University of California at Los Angeles, 607 Charles E. Young Drive East, Los Angeles, California 90095, United States

[‡]Laboratoire Kastler Brossel, Ecole Normale Supérieure, Université Pierre et Marie Curie — Paris 6

Supporting Information

ABSTRACT: We present a robust scheme for preparation of semiconductor quantum dots (QDs) and cognate partners in a conjugation ready format. Our approach is based on bis-aryl hydrazone bond formation mediated by aromatic aldehyde and hydrazinonicotinate acetone hydrazone (HyNic) activated peptide coated quantum dots. We demonstrate controlled preparation of antibody—QD bioconjugates for specific targeting of endogenous epidermal growth factor receptors in breast cancer cells and for single QD tracking of transmembrane proteins via an extracellular epitope. The same approach was also used for optical mapping of RNA polymerases bound to combed genomic DNA in vitro.

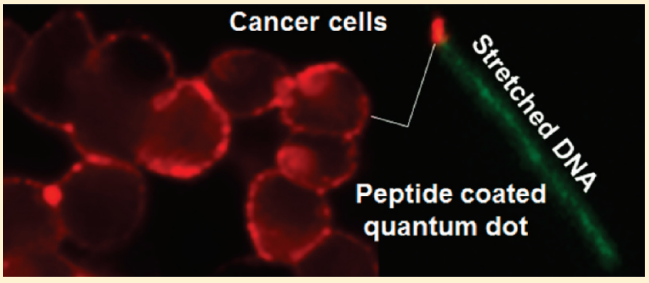

Biofunctionalization of quantum dots (QDs) for both *in vitro* and *in vivo* applications is challenging, since many criteria, such as long-term stability, overall size, efficient and straightforward conjugation of functional biomolecules, and easy QDs targeting to cellular components all have to be simultaneously optimized. We have previously developed a compact surface coating chemistry that employs synthetic peptides for solubilization, biofunctionalization, and long-term stabilization of colloidal QD solutions (>6 month).[1,2] These peptide coated QDs (pcQDs) have been targeted in cells and animals using various small functional groups such as biotin,[2,3] FITC,[4] or DOTA.[5,6] The results have provided ample proof of pcQDs advantages for both live cell single molecule imaging[7] and whole animal imaging applications. However, as recently demonstrated by the monofunctional conjugation of avidin to pcQDs[7] conjugation of large molecules to QDs is still challenging because steric hindrance, geometry, stoichiometry of the conjugate, and its final functional activity have to be addressed. For that reason, we have focused our efforts here on developing "conjugation-ready" pcQDs that are stable at 4 °C for >4—6 months and provide a flexible approach for rapid bioconjugation to antibodies and other biomolecules in aqueous buffers and with precise and reproducible control over the conjugate stoichiometry. Previously, commercial linkers and activators have been used for various types of pcQD conjugation reactions with mixed success. For instance, cetuximab, a clinical anti-EGFR (epidermal growth factor receptor) antibody conjugated to QDs via EDC (1-ethyl-3-(3 dimethylaminopropyl) carbodiimide hydrochloride) was observed to have low reactivity and the QD conjugates were prone to aggregation.[8] Alternative QD—cetuximab conjugation strategies using succinimidyl-4-(*N*-maleimidomethyl)cyclohexane-1-carboxylate (SMCC) or *N*-succinimidyl-6-(3′-(2-pyridyldithio)-propionamido)-hexanoate LC-(SPDP)/SMCC linkers were more successful but required multiple preparative steps and reduction of the antibody which could compromise its activity.[8]

To overcome some of these limitations, we developed a bis-aryl hydrazone linkage strategy for the coupling of pcQDs to antibodies. We demonstrate the utility of this approach in live cells labeling and for in *vitro* applications. This reaction is based on the bio-orthogonal stable Schiff base mediated conjugation between aromatic aldehydes and aromatic hydrazines.[9−11]

In this scheme, UV traceable bifunctional linkers, succinimidyl-4-formylbenzamide (NHS-FB) or pentafluorophenyl-poly(ethylene glycol)-4-formylbenzamide (PF-PEG-FB) and succinimidyl-6-hydrazinonicotinate acetone hydrazone (NHS-HyNic) were conjugated to pcQD and antibodies, respectively, and further reacted together to yield stable QD conjugates via the formation of a covalent bis-aryl hydrazone bond with virtually no competing side reactions (Scheme 1). These linkers can be used interchangeably on pcQDs and antibodies or other biomolecules without a loss of generality, yield, or stability. Bis-aryl hydrazone bond formation can also be catalyzed and reaction kinetics improved 10—100-fold in the pH range 5—8 in the presence of aniline.[12−14] The reaction of

Received: January 18, 2011
Revised: May 6, 2011
Published: May 10, 2011

Scheme 1. Preparation of Aromatic Benzaldehyde Capped CdSe/ZnS Peptide Coated QDs and Aromatic Hydrazine Functionalized Antibodies[a]

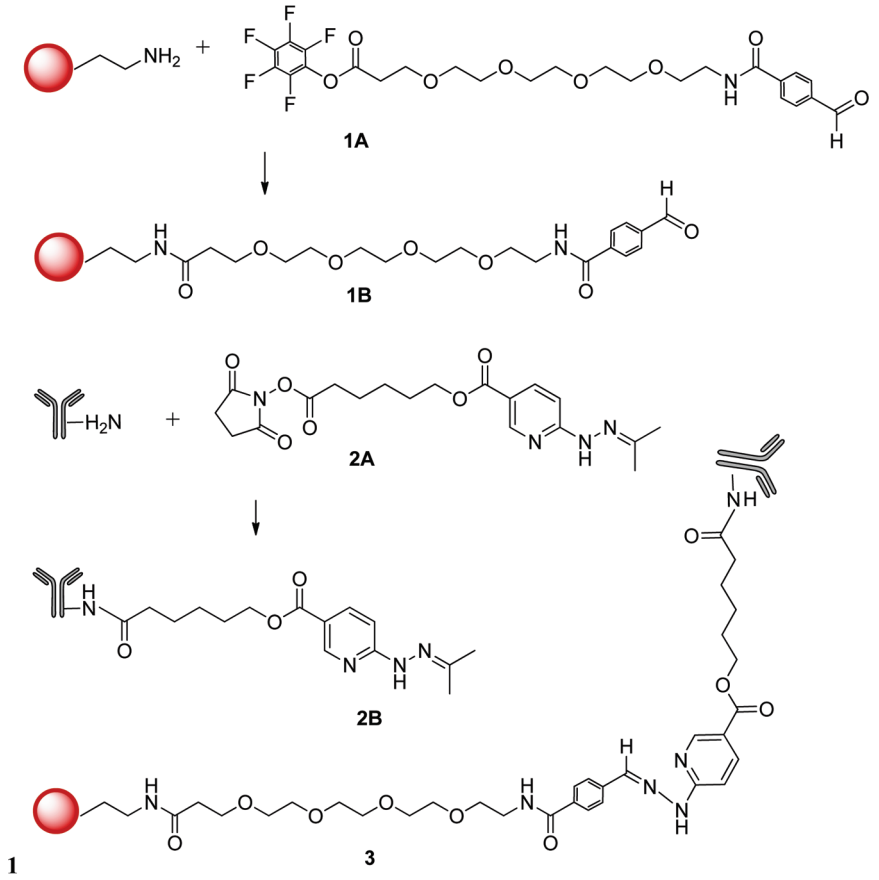

[a] Not to scale. Peptide coated quantum dots (pc-QDs) are modified with PEG-4FB, **1A**, via their primary amines to yield PEG-4FB-pcQDs, **1B**. Antibodies are modified with C6-SANH, **2A**, via surface exposed primary amines to yield C6-SANH-Abs, **2B** (nucleophilic aromatic hydrazine is protected as an acetone hydrazone); **1B** is conjugated to **2B** to form a pc-QD-Abs, **3**, bioconjugate via stable uv-traceable bis-aryl hydrazone linkage.

aromatic aldehyde with aromatic hydrazine is also completely bioorthogonal, as the functional linkers do not cross-react with other side groups present in the side chains of natural amino acids or oligonucleotides. To provide additional flexibility and control for conjugation, QDs were also coated with peptides directly synthesized with an N-terminal HyNic group. This approach saves an extra step for the preparation of reactive pcQDs and permits better control of the number of HyNic reactive groups available at the surface of QDs using mixture of peptides with different functionalities during the coating procedure.[1,2]

CdSe/CdS/ZnS QDs emitting at 630 nm (Supporting Information Figure S.1) were synthesized as described previously.[15] CdSe/ZnS QDs emitting at 605 nm were obtained in their hydrophobic form from commercial vendors. Both types of QDs were coated with glycine or lysine N-terminated synthetic peptides which resulted in available primary amines[1,2] for NHS-FB or PF-PEG-FB modifications of pcQD (see Supporting Information methods for peptide sequences). For the production of hydrazine functionalized QDs, QDs were directly coated with HyNic N-terminated synthetic peptides (HyNic-pcQD). The mean core/shell diameter of these 630 or 605 nm red-emitting QDs was ~7.5 nm and ~5.0 nm, respectively, based on TEM measurements[16] (Supporting Information Figure S.1) and their hydrodynamic diameter increased to ~12.0 nm and ~9.5 nm, respectively, once coated with peptides.[17]

Scheme 1 illustrates one approach for the conjugation of pcQDs to antibodies via bis-aryl hydrazone linkage. NHS-FB or PF-PEG-FB (**1A**) were mixed with amine terminated pcQDs either in DMSO or directly in aqueous buffer at pH 7.2 to obtain pcQDs activated with FB or with PEG-FB which further enhances the solubility pcQDs. The resulting FB-activated pcQDs (**1B**) were purified via gel filtration using water as mobile phase and rapidly exchanged into a 100 mM Na-phosphate, 150 mM NaCl, pH 6.0 conjugation buffer in which they were reactive and stable for more than 6 months when kept at 4 °C. To generate a cognate aromatic hydrazine reactive molecule, NHS-HyNic (**2A**) was similarly reacted with amine groups on anti-EGFR or anti-GFP antibodies to obtain HyNic-activated antibodies (**2B**). Once desalted into a buffer containing 100 mM Na phosphate, 150 mM NaCl, pH 6.0, HyNic-activated antibodies possessed surface exposed alkyl hydrazones that maintained a dynamic equilibrium between alkyl protecting groups and reactive hydrazine groups[18] primed to receive FB-activated pcQDs and to yield a stable QD-antibody conjugate (**3**). The QD-antibody conjugate was stored in 0.01% Tween-20 and 0.1% BSA at 4 °C. The functional stability of the conjugate was confirmed by labeling EGFR on the cell surface of live MCF-7 cells two months after 4 °C storage. It is important to note that QD-conjugates prepared using this method should be stored undiluted in micromolar concentrations.

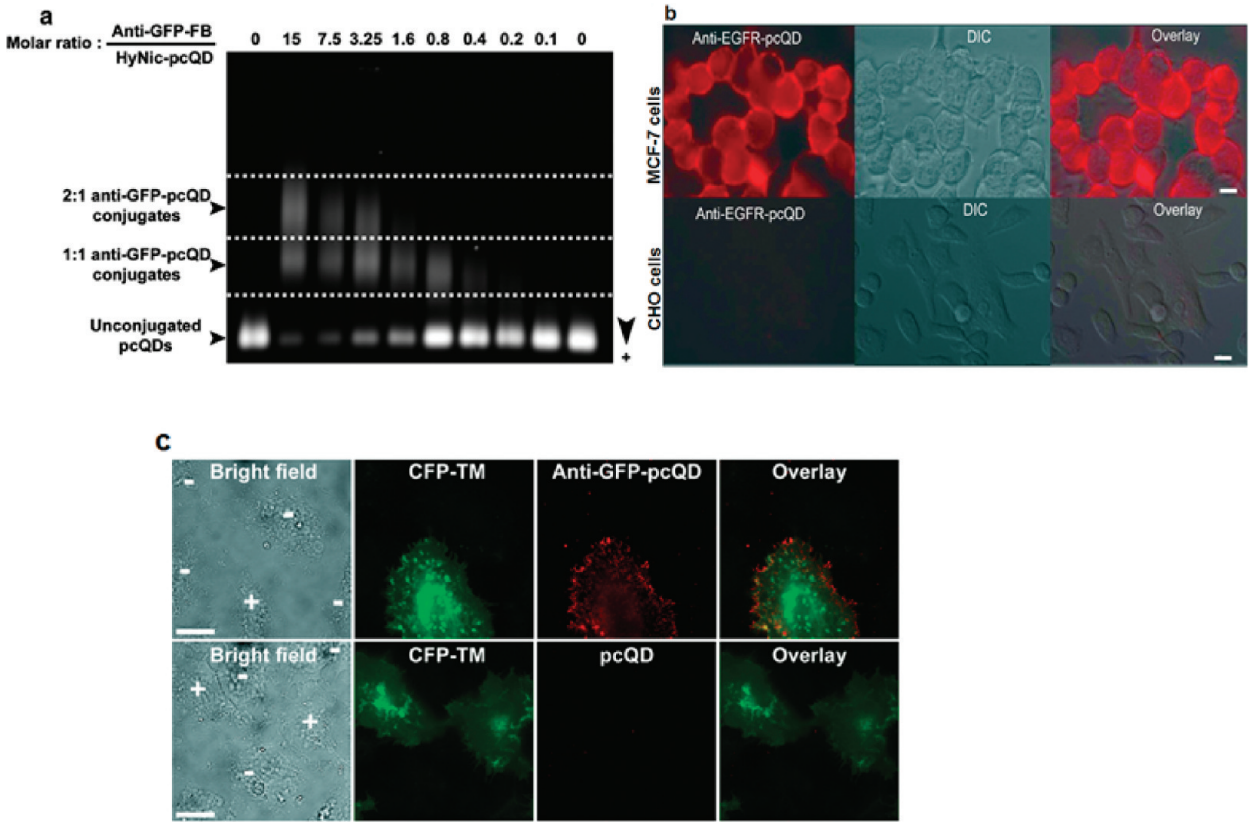

Figure 1. Cell labeling with antibody−peptide quantum dots conjugates formed by bis-aryl hydrazone linkage chemistry. (a) Gel electrophoresis of conjugation reactions between anti-GFP-FB and HyNic-pcQDs at different molar ratio. The faster migrating unconjugated HyNic-pcQD fluorescence band is depleted with increasing conjugation ratio, and discrete 1:1 and 2:1 stoichiometry anti-GFP-pcQD conjugate bands migrating more slowly in the gel appear. The side arrow indicates the direction of the electric field. (b) Labeling of live breast cancer cells MCF-7 overexpressing EGFR at the plasma membrane showing specificity with anti-EGFR-pcQD conjugate (top left); DIC image (top center) and overlay (top right). Corresponding labeling of nonexpressing EGFR live CHO cells shows no binding of anti-EGFR-pcQDs as seen in bottom right and overlay. Scale bar: 5 μm. (c) Labeling of live HeLa cells with anti-GFP-pcQD conjugates formed by the reaction of HyNic-activated anti-GFP IgG with FB-activated pcQDs (top) or with unconjugated FB-activated pc-QDs (bottom). Anti-GFP-pcQD conjugates specifically bind the plasma membrane of HeLa cell expressing a transmembrane CFP-TM receptor (+) with little nonspecific binding to nonexpressing cells (−). In the absence of antibody conjugation, no labeling to expressing cells was observed. Scale bars: 20 μm.

While generating the complementary and reactive QD (**1B**) and antibody (**2B**) species, it was important to validate the presence and to quantify the respective cross-linkers on the QDs and the antibodies. This was done using absorbance spectroscopy (Supporting Information Figure S.2) followed by a calculation of the molar substitution ratios (MSR) of each reaction. The presence and quantity of FB or HyNic groups on the surface of pcQDs and on secondary antimouse $F(ab)_2$ antibodies (used as substitutes to the more expensive anti-EGFR or anti-GFP antibodies) were measured by monitoring the increase in absorbance at 350 and 390 nm. No further increase in absorbance was observed after 100 min of reaction (Supporting Information Figure S2). The MSR of FB-activated pcQDs and HyNic-activated $F(ab)_2$ antibodies was calculated to be 10 and 1.15, respectively. In general, increasing the linker concentration beyond a maximum of 20 mol equiv for NHS-FB, PF-PEG-FB, or NHS-HyNic resulted in precipitation of the antibodies or pcQDs. For the conjugation of anti-EGFR antibodies to pcQDs, the reaction was optimized using PEG-FB-pcQDs and HyNic-modified anti-EGFR at a 1:4 molar ratio. For conjugation to anti-GFP, a 1:10 molar ratio of FB-pcQDs to HyNic-modified anti-GFP antibodies was used. When reactive groups were reversed, for instance, using HyNic-pcQD and FB-activated anti-GFP antibodies, the reaction ratio was optimized by gel electrophoresis. As shown in Figure 1a, the conjugation efficiency increased with increasing anti-GFP-FB:HyNic-pcQD ratios and was characterized by the depletion in unconjugated HyNic-pcQD fluorescent bands and the appearance of discrete and gel-shifted anti-GFP-pcQDs 1:1 and 2:1 conjugate bands. The distribution of stoichiometries (of anti-GFP-pcQDs and free pcQDs) was in good agreement with the expected Poisson distribution as previously observed for monofunctional bioconjugation of pcQD[17] (Supporting Information Figure S.3).

To demonstrate the activity of the different antibody-pcQD conjugates obtained by bis-aryl hydrazone chemistry, we tested their ability to specifically recognize membrane bound antigens in living cells. EGFR, which is often overexpressed on the cell surface in several cancers is a potential target for clinical therapy, was specifically recognized by anti-EGFR-pcQD conjugates in live MCF-7 breast cancer cells (Figure 1b) and in live U87 human glioblastoma cells (Supporting Information Figure S.4). No cell membrane staining was observed for CHO cells (Figure 1b) that do not express EGFR. An overlay of the fluorescent and DIC channel clearly confirmed the localization of the anti-EGFR-pcQD

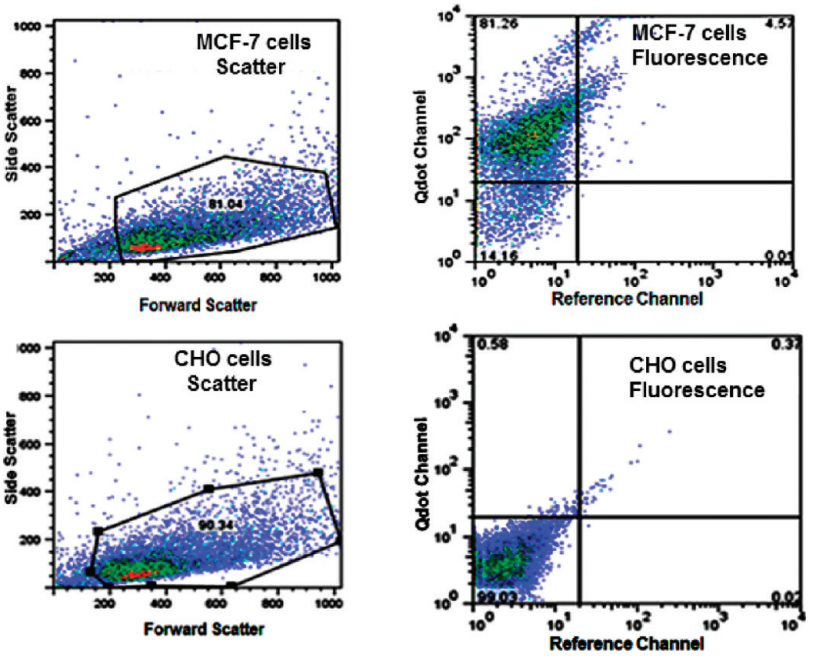

Figure 2. Flow cytometry analysis of live MCF-7 and CHO cells labeled with anti-EGFR-pcQDs. Top panel shows specific binding of 25 nM of anti-EGFR-pcQD conjugates to MCF-cells overexpressing EGFR while the bottom panel shows absence of binding to EGFR negative CHO cells at a similar concentration.

conjugates on the cell surface of cancer cells (Figure 1b), and the limited nonspecific binding observed was likely due to the presence of PEG in the linker. Similar results were obtained with anti-GFP-pcQD conjugates that specifically cross-reacted with cyan fluorescent protein (CFP) fused to the transmembrane domain of the platelet-derived growth factor receptor (CFP-TM) when expressed in the plasma membrane of HeLa cells (Figure 1c, Supporting Information Figure S.5). Again, minor nonspecific binding to nonexpressing cells was observed and cells were not labeled with unconjugated pc-QDs (Figure 1c, Supporting Information Figure S.5). Single QD tracking of CFP-TM receptors in the plasma membrane of live HeLa cells could be achieved using monofunctional anti-GFP-pcQD conjugates (Supporting Information video 1). When delivered within the cytoplasm of living cells, for instance, using INFLUX pinocytic loading[19] anti-GFP-pcQD conjugates also efficiently targeted intracellular GFP fusion proteins such as the integral membrane anchored caveolin-1-GFP (Supporting Information Figure S.6, video 2).

To extend the utility of anti-EGFR-pcQD conjugates, in particular, for immunophenotyping experiments,[20] titration and binding efficiencies were compared for EGFR overexpressing MCF-7 breast cancer cells versus nonexpressing CHO cells by flow cytometry measurements (Figure 2, Supporting Information Figure S.7). More than 80% of MCF-7 cells were fluorescent when stained with a 25 nM concentration of anti-EGFR-pcQD, while less than 1% CHO cells were labeled under the same conditions (Figure 2). Control experiments with pcQD reacted with a normal mouse IgG_{2a} isotypic antibody (25 nM IgG_{2a}-pcQDs) via the same bis-aryl hydrazone conjugation strategy showed an absence of cell surface staining for both MCF-7 and CHO cell lines (Supporting Information Figure S.8). The combined results from fluorescence microscopy and flow cytometry experiments clearly demonstrate the utility of this bis-aryl hydrazone conjugation chemistry for the production of relatively small size, active antibody-QD conjugates. In addition to pcQDs,

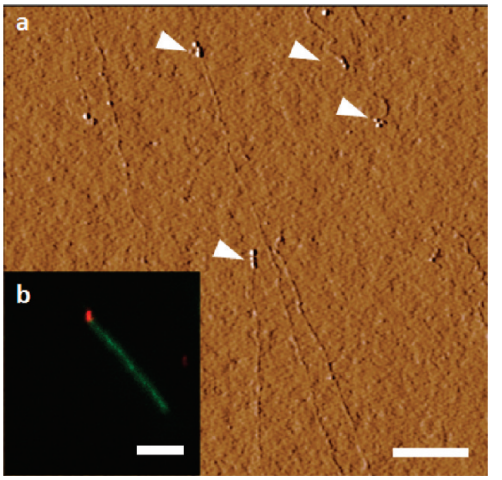

Figure 3. *In vitro* detection of DNA binding proteins using antiRNAP-pcQDs. (a) AFM height image of extended T7 bacteriophage DNA reacted with *E. coli* RNAPs. The protrusions at the end of the DNA fiber (arrows) confirm specific binding of RNAPs to their expected location on the T7 genome. Scale bar 1 μm. (b) Fluorescence image of the same sample after incubation with pcQDs conjugated to antibodies against *E. coli* RNAP allows specific QD recognition of RNAP on the T7 genome. Scale bar 5 μm.

commercial amine-PEG-545 nm and amine-coated 611 nm QDs (Life Technologies or eBioscience) conjugated to antibodies via the same bis-aryl hydrazone linkage showed similar conjugation kinetics and labeling efficiency in living cells, although their larger size compared to pcQDs prevented the isolation of antibody-QD conjugates with well-defined stoichiometry (unpublished results).

To further demonstrate the utility of bis-aryl hydrazone linked antibody-pcQD conjugates, we employ them for an *in vitro* optical imaging application. The detection of *E. coli* RNA polymerases

(RNAPs) interacting with T7 bacteriophage genomic DNA combed on glass surfaces was taken as a model system. *E. coli* RNAPs strongly interact with binding sites (promoters) in the first 750 base pairs of the T7 genome[21] as confirmed by atomic force microscopy (AFM) imaging[22] (Figure 3a). For optical detection of RNAPs along the T7 genome, hydrophobic QDs emitting at 605 nm were coated with peptides described above and conjugated to antibodies directed against the β subunit of *E. coli* RNAP. The anti-RNAP-pcQD conjugates were reacted with the T7-genome/RNAP complex and the sample was stretched on a polylysine modified glass coverslip after staining with YoYo-1, a DNA intercalating dye (Life Technologies). When the complexes were imaged by fluorescence microscopy, anti-RNAP-pcQDs (Figure 3b, red) were detected at the extremity of the T7-genomic DNA (Figure 3b, green), an indication of effective and specific RNAP targeting *in vitro*.

A substantial body of work related to hydrazone bonds have been implemented for a variety of pH-sensitive conjugates of anticancer drug doxorubicin with antibodies, polymers, micelles, and particles.[23,24] The stability of certain types of hydrazone linkers is well documented at 7.4, while at a lower pH 5.0 these linkers undergo hydrolysis.[23,25] Few examples of hydrazone linker technology incorporated in antibody drug conjugates are as follows: (i) Mylotarg,[26] (ii) the antibody−calicheamicin conjugate,[27] and (iii) CMC-544, a promising drug−antibody conjugate—N-acetyl γ calicheamicin dimethylhydrazide (CalichDMH) conjugated to humanized anti-CD22 monoclonal antibody.[28] While Mylotarg was recently withdrawn from the market by FDA due to fatalities reported in humans, CMC-544 is currently being evaluated in a phase III study for the treatment of B-lymphoid malignancies. Both drugs have incorporated the concept of acid hydrolyzable linker which is different from the aromatic bis-aryl hydrazone conjugate used in this study. The aromatic bis-aryl hydrazone is more stable in the pH range 5−8 relevant to *in vitro* and cell surface labeling experiments. It would therefore be interesting to test in the future the efficacy and stability of the bis-aryl hydrazone linker technology in preclinical settings in mice.

There are several advantages to the aromatic aldehyde-hydrazone QD conjugation strategy described here. First, FB-pcQDs, PEG-FB-pcQDs, or HyNic-pcQDs obtained after purification of the linkers or removal of excess coating peptides, can be stored for 4−6 months at 4 °C with minimal loss in activity. Second, proteins or other biomolecules conjugated with either of these linkers can themselves be conserved for extensive periods by freezing. Third, the internal UV traceable markers built in both types of linkers allows for easy monitoring and control of the MSR when modifying QDs or proteins. Fourth, bioconjugation only requires mixing the two active (QD and protein) components and the reaction efficiency of bis-aryl hydrazone formation can be further improved in the presence of aniline.[11,12,29,30] In this context, a method for controlled assembly of QD-biomolecule hybrids using aniline catalyzed hydrazone ligation has been successfully demonstrated.[31] Further utility of the aniline catalyzed hydrazone reaction has been shown for attaching protein capture reagents to model silicon dioxide surface suggesting that it can be used for biosensor applications in the biomedical field.[32] Fifth, the small size of pcQDs and that of the antibody-pcQD conjugates allows for an easy production and purification of monofunctional conjugates and antibody-pcQDs with well-defined stoichiometry. Sixth, the bioorthogonal reactivity of the bis-aryl hydrazone linkage should favor the control grafting of multiple proteins or reactive moieties on the surface of individual pcQD, and should facilitate the production of multifunctional QD probes. Finally, for bioorthogonal site-specific targeting and imaging in living cells, a formylglycine aldehyde tag[33,34] can be genetically engineered into proteins, which can be potentially targeted via hydrazone activated pc-QDs.

■ ASSOCIATED CONTENT

Supporting Information. Additional figures and methods as described in text. Experimental procedures, synthesis of quantum dots, UV−vis kinetics of conjugation and titration of bioconjugates using flow cytometry, stoichiometry of antibody binding to QDs using gel electrophoresis and fluorescence microscopy. This material is available free of charge via the Internet at http://pubs.acs.org.

■ AUTHOR INFORMATION

Corresponding Author

*E-mail: gopal@chem.ucla.edu; fabien.pinaud@lkb.ens.fr; sweiss@chem.ucla.edu.

Author Contributions

§These authors contributed equally.

■ ACKNOWLEDGMENT

We thank Jieun Choi for recording absorbance measurements using UV−vis spectroscopy and David Schwartz (SoluLink Biosciences, Inc.) for critical reading of the manuscript. Electron microscopy was performed at the Electron Imaging Center for Nanomachines (EICN) at the UCLA/California Nanosystems Institute (CNSI) core facility. We acknowledge UCLA Jonsson Comprehensive Cancer Center (JCCC) and Center for AIDS Research Flow Cytometry Core Facility that is supported by National Institutes of Health awards CA-16042 and AI-28697, and by the Johsson Cancer Center, the UCLA AIDS Institute, and the David Geffen School of Medicine at UCLA. Fluorescence imaging was performed at the UCLA/CNSI Advanced Light Microscopy Shared Facility. This work was supported by NIH/NIBIB BRP Grant R01-EB000312 and the NSF, The Center for Biophotonics, an NSF Science and Technology Center managed by the University of California, Davis, under Cooperative Agreement PHY0120999. F.P. acknowledges financial support from a Marie Curie-Intra-European Fellowship under contract number MEIF-CT-2006-040210, an EMBO long-term fellowship, and a fellowship from Centre de Nanoscience Ile de France. M.D. acknowledges support from Fondation pour la Recherche Médicale."

■ REFERENCES

(1) Iyer, G., Pinaud, F., Tsay, J., and Weiss, S. (2007) Solubilization of quantum dots with a recombinant peptide from Escherichia coli. *Small 3*, 793–798.

(2) Pinaud, F., King, D., Moore, H. P., and Weiss, S. (2004) Bioactivation and cell targeting of semiconductor CdSe/ZnS nanocrystals with phytochelatin-related peptides. *J. Am. Chem. Soc. 126*, 6115–23.

(3) Pinaud, F., Michalet, X., Iyer, G., Margeat, E., Moore, H.-P., and Shimon, W. (2009) Dynamic partitioning of a glycosyl-phosphatidylinositol-anchored protein in glycosphingolipid-rich microdomains imaged by single-quantum dot tracking. *Traffic 10*, 691–712.

(4) Iyer, G., Michalet, X., Chang, Y.-P., Pinaud, F. F., Matyas, S. E., Payne, G., and Weiss, S. (2008) High affinity scfvâ'hapten pair as a tool

for quantum dot labeling and tracking of single proteins in live cells. *Nano Lett. 8*, 4618–4623.

(5) Schipper, M. L., Iyer, G., Koh, A. L., Cheng, Z., Ebenstein, Y., Aharoni, A., Keren, S., Bentolila, L. A., Li, J., Rao, J., Chen, X., Banin, U., Wu, A. M., Sinclair, R., Weiss, S., and Gambhir, S. S. (2009) Particle size, surface coating, and pegylation influence the biodistribution of quantum dots in living mice. *Small 5*, 126–134.

(6) Schipper, M. L., Cheng, Z., Lee, S.-W., Bentolila, L. A., Iyer, G., Rao, J., Chen, X., Wu, A. M., Weiss, S., and Gambhir, S. S. (2007) microPET-based biodistribution of quantum dots in living mice. *J. Nucl. Med. 48*, 1511–1518.

(7) Pinaud, F., Clarke, S., Sittner, A., and Dahan, M. (2010) Probing cellular events, one quantum dot at a time. *Nat. Methods 7*, 275–285.

(8) Lee, J., Choi, Y., Kim, K., Hong, S., Park, H.-Y., Lee, T., Cheon, G. J., and Song, R. (2010) Characterization and cancer cell specific binding properties of Anti-EGFR antibody conjugated quantum dots. *Bioconjugate Chem. 21*, 940–946.

(9) Yuan, Q., Yeudall, W. A., and Yang, H. (2010) PEGylated polyamidoamine dendrimers with bis-aryl hydrazone linkages for enhanced gene delivery. *Biomacromolecules 11*, 1940–1947.

(10) Kozlov, I. A., Melnyk, P. C., Stromsborg, K. E., Chee, M. S., Barker, D. L., and Zhao, C. (2004) Efficient strategies for the conjugation of oligonucleotides to antibodies enabling highly sensitive protein detection. *Biopolymers 73*, 621–630.

(11) Prasuhn, D. E., Blanco-Canosa, J. B., Vora, G. J., Delehanty, J. B., Susumu, K., Mei, B. C., Dawson, P. E., and Medintz, I. L. (2010) Combining chemoselective ligation with polyhistidine-driven self-assembly for the modular display of biomolecules on quantum dots. *ACS Nano 4*, 267–278.

(12) Dirksen, A., and Dawson, P. E. (2008) Rapid oxime and hydrazone ligations with aromatic aldehydes for biomolecular labeling. *Bioconjugate Chem. 19*, 2543–2548.

(13) Grotzky, A., Manaka, Y., Kojima, T., and Walde, P. (2010) Preparation of catalytically active, covalent α-polylysine−enzyme conjugates via UV/vis-quantifiable bis-aryl hydrazone bond formation. *Biomacromolecules 12*, 134–144.

(14) Dirksen, A., Yegneswaran, S., and Dawson, P. E. (2010) Bisaryl hydrazones as exchangeable biocompatible linkers. *Angew. Chem., Int. Ed. 49*, 2023–2027.

(15) Li, J. J., Wang, Y. A., Guo, W., Keay, J. C., Mishima, T. D., Johnson, M. B., and Peng, X. (2003) Large-scale synthesis of nearly monodisperse CdSe/CdS core/shell nanocrystals using air-stable reagents via successive ion layer adsorption and reaction. *J. Am. Chem. Soc. 125*, 12567–12575.

(16) Clarke, S., Pinaud, F., Sittner, A., Gouzer, G., Beutel, O., Piehler, J., and Dahan, M. (2010) Monofunctional quantum dot probes for single-molecule imaging. *Biophys. J. 98*, 403a–403a.

(17) Clarke, S., Pinaud, F., Beutel, O., You, C., Piehler, J., and Dahan, M. (2010) Covalent monofunctionalization of peptide-coated quantum dots for single-molecule assays. *Nano Lett. 10*, 2147–2154.

(18) Schwartz, D. A., Abrams, M. J., Hauser, M. M., Gaul, F. E., Larsen, S. K., Rauh, D., and Zubieta, J. A. (1991) Preparation of hydrazino-modified proteins and their use for the synthesis of technetium-99m-protein conjugates. *Bioconjugate Chem. 2*, 333–336.

(19) Okada, C. Y., and Rechsteiner, M. (1982) Introduction of macromolecules into cultured mammalian cells by osmotic lysis of pinocytic vesicles. *Cell 29*, 33–41.

(20) Chattopadhyay, P. K., Price, D. A., Harper, T. F., Betts, M. R., Yu, J., Gostick, E., Perfetto, S. P., Goepfert, P., Koup, R. A., De Rosa, S. C., Bruchez, M. P., and Roederer, M. (2006) Quantum dot semiconductor nanocrystals for immunophenotyping by polychromatic flow cytometry. *Nat. Med. 12*, 972–977.

(21) Dunn, J. J., and Studier, F. W. (1983) Complete nucleotide sequence of bacteriophage T7 DNA and the locations of T7 genetic elements. *J. Mol. Biol. 166* (4), 477–535.

(22) Ebenstein, Y., Gassman, N., Kim, S., Antelman, J., Kim, Y., Ho, S., Samuel, R., Michalet, X., and Weiss, S. (2009) Lighting up individual DNA binding proteins with quantum dots. *Nano Lett. 9*, 1598–1603.

(23) Senter, P. D., and Meyer, D. L. (2007) Monoclonal antibody drug conjugates for cancer therapy, in *Prodrugs* (Stella, V. J., Borchardt, R. T., Hageman, M. J., Oliyai, R., Maag, H., and Tilley, J. W., Eds.) pp 507−524, Springer, New York.

(24) McCarron, P. A., Olwill, S. A., Marouf, W. M. Y., Buick, R. J., Walker, B., and Scott, C. J. (2005) Antibody conjugates and therapeutic strategies. *Mol. Interventions 5*, 368–380.

(25) Mahato, R., Tai, W., Cheng, K. Prodrugs for improving tumor targetability and efficiency. *Adv. Drug Delivery Rev.* In Press.

(26) Sievers, E. L. (2003) Antibody-targeted chemotherapy of acute myeloid leukemia using gemtuzumab ozogamicin (Mylotarg). *Blood Cells, Molecules, and Diseases 31*, 7–10.

(27) Alley, S. C., Okeley, N. M., and Senter, P. D. (2010) Antibody-drug conjugates: targeted drug delivery for cancer. *Curr. Opin. Chem. Biol. 14*, 529–537.

(28) Wong, B. Y., and Dang, N. H. (2010) Inotuzumab ozogamicin as novel therapy in lymphomas. *Expert Opin. Biol. Ther. 10*, 1251–1258.

(29) Dirksen, A., Dirksen, S., Hackeng, T. M., and Dawson, P. E. (2006) Nucleophilic catalysis of hydrazone formation and transimination: implications for dynamic covalent chemistry. *J. Am. Chem. Soc. 128*, 15602–15603.

(30) Dirksen, A., Hackeng, T. M., and Dawson, P. E. (2006) Nucleophilic catalysis of oxime ligation. *Angew. Chem., Int. Ed. 45*, 7581–7584.

(31) Blanco-Canosa, J. B., Medintz, I. L., Farrell, D., Mattoussi, H., and Dawson, P. E. (2010) Rapid covalent ligation of fluorescent peptides to water solubilized quantum dots. *J. Am. Chem. Soc. 132*, 10027–10033.

(32) Byeon, J.-Y., Limpoco, F. T., and Bailey, R. C. (2010) Efficient bioconjugation of protein capture agents to biosensor surfaces using aniline-catalyzed hydrazone ligation. *Langmuir 26*, 15430–15435.

(33) Rush, J. S., and Bertozzi, C. R. (2008) New aldehyde tag sequences identified by screening formylglycine generating enzymes in vitro and in vivo. *J. Am. Chem. Soc. 130*, 12240–12241.

(34) Frese, M. A., and Dierks, T. (2009) Formylglycine aldehyde tag—protein engineering through a novel post-translational modification. *ChemBioChem 10*, 425–427.